www.czasopisma.pan.pl PAN www.journals.pan.pl

Acta Geologica Polonica, Vol. 75 (2025), No. 1, e36

DOI: 10.24425/agp.2024.151758

Are quick equivalent doses realistic? Testing range-finder luminescence dating for water-lain and postglacial flooding sediments in NE Poland

EDYTA KALIŃSKA[1], HELENA ALEXANDERSON[2], PIOTR WECKWERTH[1], JAN A. PIOTROWSKI[1,3] and WOJCIECH WYSOTA[1]

[1] *Nicolaus Copernicus University in Toruń, Faculty of Earth Sciences and Spatial Management, Lwowska 1, 87-100 Toruń, Poland; e-mails: edyta.kalinska@umk.pl; pweck@umk.pl; jan.piotrowski@umk.pl*

[2] *Lund University, Department of Geology, Sölvegatan 12, 223 62 Lund, Sweden; e-mail: helena.alexanderson@geol.lu.se*

[3] *Aarhus University, Department of Geoscience, Høegh-Guldbergs Gate 2, DK-8000 Aarhus C, Denmark; e-mail: jan.piotrowski@geo.au.dk*

ABSTRACT:

Kalińska, E., Alexanderson, H., Weckwerth, P., Piotrowski, J.A. and Wysota, W. 2025. Are quick equivalent doses realistic? Testing range-finder luminescence dating for water-lain and postglacial flooding sediments in NE Poland. *Acta Geologica Polonica*, **75** (1), e36.

Raw sediment samples which are without prior lengthy laboratory preparation can be used to obtain a rough but rapid estimate of the luminescence equivalent dose, and thus of the relative age of the sediment. In this study, we tested this range-finder method on clastic sediments in NE Poland for the first time, with special focus on Pleistocene meltwater sediments generated by highly energetic glacial lake outburst floods, and the post-flooding sediments. Two datasets with known doses from standard measurements were compared to range-finder doses determined from quartz and feldspar in untreated sediments. We found statistically significant correlation between equivalent doses of (1) standard quartz optically stimulated luminescence (OSL) and range-finder feldspar infrared stimulated luminescence (IRSL) at 50 ºC, and (2) standard quartz OSL and range-finder quartz OSL in low-dose samples (<80 Gy). However, these correlations should only be considered as approximate whereby preparing more than three range-finder aliquots has the potential of yielding more accurate results. Correlation between the range-finder quartz OSL and range-finder feldspar IRSL is also significant. The range-finder measurements can be used for approximate dose determination to preliminary assess the sediment age or as a selection tool to avoid incompletely bleached samples. The sedimentary environment and especially sediment reworking and transportation seem to influence these correlations. We consider the sediments studied here to have undergone between one and four reworking stages, and samples with repeated reworking usually represent well-bleached material for luminescence dating.

Key words: Luminescence dating, equivalent dose; Glacial lake outburst flood (GLOF) sediments; Aeolian sediments; Sand-wedge sediments.

INTRODUCTION

Optically stimulated luminescence (OSL) is a commonly used method to determine the depositional age of sediments and an increase in studies on OSL signals, doses and ages over the past decade (e.g. Wintle and Adamiec 2017; Mahan *et al.* 2023). Although widely used, OSL dating is time-consuming and expensive due to labour-intensive sample preparation, long measurement times, and the need for specialized equipment. Roberts *et al.* (2009) estimated the required time to be typically 2–6 months from sample collection to the calculation of an OSL age, and between somewhere around two and several weeks for comprehensive laboratory preparation and measurement. In OSL dating studies that include sediments that may be problematic, e.g. due to depositional process or material characteristics, it would be valuable to pick out those sediments or samples that are most likely to give useful results by some advance information about the samples. Consideration of the sedimentology and geomorphology is critical for taking the most suitable samples (e.g. King *et al.* 2014a, b; Weckwerth *et al.* 2013), but sometimes what is 'best' is not obvious from properties visible in the field.

This is the case in north-eastern Poland where water-lain sediments have recently been mapped (Weckwerth *et al.* 2019, 2022) and linked to highly energetic Pleistocene glacial lake outburst floods (GLOFs; Carling 2013). These sediments constitute a complex suite of proglacial landforms including vast outwash plains (i.e., the Augustów Plain, Text-fig. 1) and megadunes (giant current dunes) and both are subject to ongoing detailed investigations (see Text-fig. 2 for OSL sampling points). Situated above the GLOF sediments, there are sediments deposited by processes other than outburst floods (e.g., in periglacial conditions; Woronko and Dąbski 2023), which can be used to constrain the terminations of flood sediments. The GLOFs are expected to have taken place during the end of the last glaciation (the Weichselian) but their exact timing is poorly known. Since the sediments contain no or only little organic matter, luminescence dating has been applied to constrain their chronology. Luminescence dating has been widely used for outburst flood sediments (Herget *et al.* 2020; Last and Rittenour 2021; Yang *et al.* 2022) but obtaining realistic ages is a challenge, because hyperconcentrated flow deposits, which are characteristic of GLOFs, commonly contain grains that did not experience sufficient exposure to sunlight during transportation (Hu *et al.* 2022) and thus suffer from incomplete bleaching (which leads to dose and age overestimation).

Age overestimation is indeed common in these Polish GLOF sediments, as shown by our attempts to date them (Weckwerth *et al.* 2024; Kalińska *et al.* in press). To improve the success rate for accurate dating, we wish to test to what extent rapid luminescence analysis of untreated material can be used

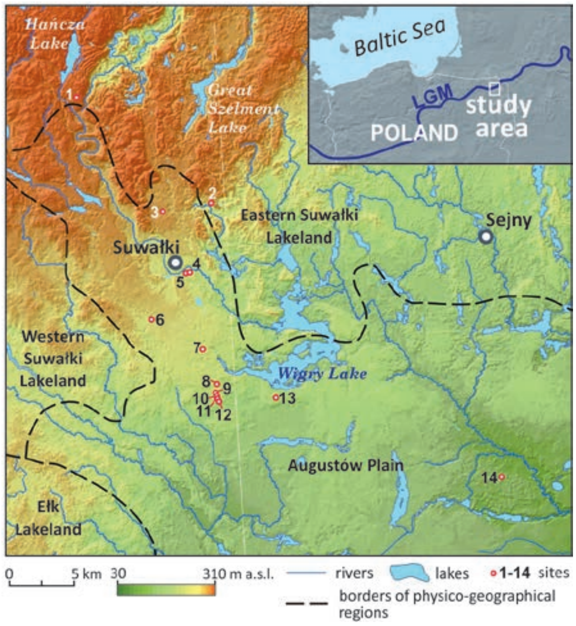

Text-fig. 1. Location and morphology of the study area with the investigated sites: 1 – Bachanowo 5; 2 – Osinki 2; 3 – Biała Woda 1; 4 – Suwałki Utrata 2; 5 – Suwałki Utrata 1; 6 – Suwałki Airfield 1; 7 – Płociczno 3; 8 – Płociczno 1; 9 – Ateny 2; 10 – Ateny 3; 11 – Ateny 1; 12 – Ateny 4; 13 – Bryzgiel 1; 14 – Płaska 2.

to assess samples prior to full analysis by providing estimates of dose and risk of incomplete bleaching.

Various approaches using rapid luminescence measurements on more or less untreated sediment – commonly called luminescence profiling or range-finder dating – have been developed and tested. This includes, for example, measuring the spatial distribution of dose results across a site with no or limited preparatory treatment (Sanderson *et al.* 2001; 2003; Burbidge *et al.* 2007; Roberts *et al.* 2009) or in-field measurement of luminescence signals in a portable luminescence reader (Sanderson and Murphy 2010; King *et al.* 2014b; Stone *et al.* 2015, 2016; Munyikwa *et al.* 2021). Single-aliquot regeneration (SAR) analytical protocols may be used, such as in the range-finder (RF) dating by Roberts et al. (2009), or other types of protocols such as the CW Proxies introduced by Sanderson and Murphy (2010). Most protocols include stimulation by both infrared and blue light to account for the mixed mineralogy of untreated samples and provides values of equivalent dose or luminescence signal strength. Pulsed OSL may additionally be applied to separate quartz and feldspar signals in a mixed quartz/feldspar sample (Denby *et al.* 2006; Thomsen *et al.* 2008).

Importantly, any RF protocol provides a rough

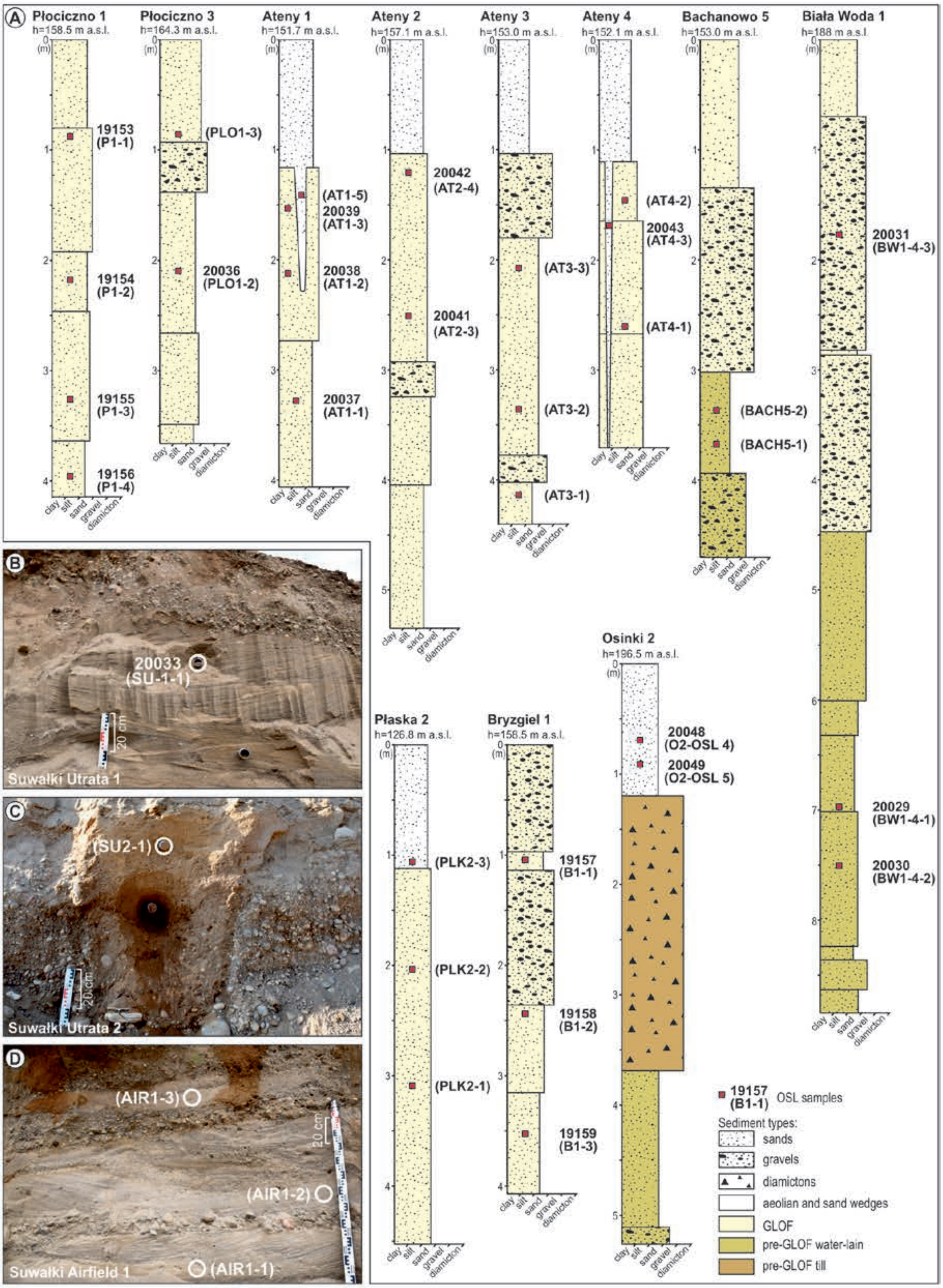

Text-fig. 2. Details of the investigated sediments. A – simplified sediment sections with pre-GLOF, GLOF, aeolian, and sand-wedge types; B – Suwałki Utrata 1 site with GLOF sediments; C – Suwałki Utrata 2 site with sand-wedge sediments; D – Suwałki Airfield 1 section with GLOF sediments.

approximation of equivalent doses only and cannot replace comprehensive laboratory preparation and measurement (Durcan *et al.* 2010) when precise results are needed. It has been determined that raw sample dose estimates can reproduce 65–70% of doses from fully prepared samples (Roberts *et al.* 2009), or even up to 96% (Alexanderson and Bernhardson 2016). However, the occurrence of feldspar often seems to hamper the correlation (accuracy), likely due to differences between quartz and feldspar in their bleaching potential and signal stability (feldspar being slower to bleach (Wallinga 2002) and suffering from fading (Wintle 1973; Spooner 1994). To estimate ages from RF doses, information on the environmental dose rate – the other factor in the age equation – is also needed. The dose rate is the rate of exposure to alpha (α), beta (β), and gamma (γ) radiation from radioisotopes of K, U, Th, Rb, and incoming cosmic rays (Murray and Wintle 2000) and is site and sample specific, but if not too variable across an area, an average from previous luminescence dating in the area can be used as a rough estimate. Ages estimated in this way have been found to be in good agreement with available independent dating evidence from radiocarbon dating (Durcan *et al.* 2010), which supports its reliability.

The aims of this study are to determine (1) to what extent RF doses can be used to estimate standard (time-consuming) doses, and (2) if RF can be used to identify poorly bleached samples. To reach these aims, we compare known doses, from standard measurements (SM-OSL), and several varieties of range-finder doses from raw sediment material, targeting luminescence signals from both quartz and feldspar. We discuss potential causes and correlations with environmental factors, such as depositional environment.

STUDY AREA

The landscape of NE Poland, with elevations between ~30 m a.s.l. in valleys and ~300 m a.s.l. in the uplands (Text-fig. 1), resulted from GLOF events during the Weichselian glaciation at around 19 ka and shortly after 16 ka (Weckwerth *et al.* 2019), in accord with the regional stratigraphy (Marks 2002; 2012; Ber 2006; Dzierżek and Zreda 2007). This landscape is particularly distinct in the Western and Eastern Suwałki Lakelands (Text-fig. 1), where subglacial and proglacial landforms occur including several meltwater drainage gates at the past ice sheet margin and proglacial spillways in more distal areas (see for details fig. 2 in Weckwerth *et al.* 2019). Further south, a vast outwash plain, the Augustów Plain, occurs with surface elevation between 120 m a.s.l. in the south-eastern and 242 m a.s.l. in the north-western part. In general, this outwash plain is a relatively flat landform except for the area next to the town of Suwałki. There, the meltwater spillways continue at several topographic levels, level 2 being the spatially most extensive. The area around Wigry Lake and further to the south-east is relatively flat but parallel megadune ridges grouped in several fields on the outwash level 2 record an impact of ice-proximal GLOFs there (Weckwerth *et al.* 2019).

MATERIAL

Thirty-six samples from fourteen sediment sections located on the Augustów Plain (Text-fig. 1) or in the nearby Eastern Suwałki Lakeland (Osinki; site 2 in Text-fig. 1) were taken for analyses. The samples represent several sediment types that belong to three stratigraphical groups (Table 1): 1) pre-GLOF sands and gravels (Bachanowo 5 and Biała Woda 1; Text-fig. 2A), 2) gravelly-sandy GLOF sediments (all sections except for Osinki 2; Text-fig. 2A–D), and 3) post-GLOF sand either of aeolian or periglacial origin (Ateny 1 and 4, Płaska 2, Osinki 2 (Text-fig. 2A), Suwałki Utrata 2 profiles (Text-fig. 2C). From their stratigraphic context and according to available datings, we expect the pre-GLOF sands to be older than 20 ka and the post-GLOF deposits of late glacial or Holocene age (<15 ka) with the GLOF deposits sandwiched between.

Range-finder doses were measured on all 36 samples. Of these, 20 samples have also been dated by standard OSL procedures (Table 2) and their equivalent doses are known (Kalińska *et al.* in press). Most samples (22; Tables 1, 2) originate from GLOFs and represent their different stages (for example, pre-flooding, maximum of flooding and waning of flooding). Two samples (20048 and -49, Osinki profile) represent dry deposition on a wet surface (so-called fluvioperiglacial sediments) on top of the glacial pre-GLOF sediments in the region (W. Wysota, pers. com.). Finally, three samples post-date GLOFs and come from sand wedges developed in GLOF sediments (Text-fig. 2C; Table 1).

METHODS

All samples were taken with ~30-cm long opaque tubes hammered in freshly cleaned walls and sealed instantly to avoid sunlight exposure. For RF measure-

Field ID	Lund ID	Profile	Landform	Type of sediment
P1-1	19153	Płociczno 1	megadune	GLOF (waning)
P1-2	19154			GLOF
P1-3	19155			GLOF
P1-4	19156			GLOF
B1-1	19157	Bryzgiel 1	megadune	GLOF
B1-2	19158			GLOF
B1-3	19159			pre-GLOF water-lain
BW1-4-1	20029	Biała Woda 1	outwash level 2	pre-GLOF water-lain
BW1-4-2	20030			pre-GLOF water-lain
BW1-4-3	20031			GLOF
SU1-1	20033	Suwałki Utrata 1	outwash level 3	GLOF
SU2-1	–	Suwałki Utrata 2	outwash level 3	sand-wedge
PLO1-2	20036	Płociczno 3	megadune	GLOF
PLO1-3	–			GLOF (waning)
AT1-1	20037	Ateny 1	megadune	GLOF
AT1-2	20038			GLOF
AT1-3	20039			GLOF (waning)
AT1-5	–			sand-wedge
AT2-3	20041	Ateny 2	megadune	GLOF
AT2-4	20042			GLOF (waning)
AT4-1	–	Ateny 4	megadune	GLOF
AT4-2	–			GLOF (waning)
AT4-3	20043			sand-wedge
O2-OSL4	20048	Osinki 2	meltwater erosion-al surface	aeolian (fluvioperiglacial)
O2-OSL5	20049			aeolian (fluvioperiglacial)
AT3-1	–	Ateny 3	megadune	GLOF
AT3-2	–			GLOF
AT3-3	–			GLOF
BACH5-1	–	Bachanowo 5	outwash level 2	pre-GLOF water-lain
BACH5-2	–			pre-GLOF water-lain
PLK2-1	–	Płaska 2	megadune	GLOF
PLK2-2	–			GLOF
PLK2-3	–			aeolian
AIR1-1	–	Suwałki Airfield 1	outwash level 2	GLOF
AIR1-2	–			GLOF
AIR1-3	–			GLOF

Table 1. Details of samples investigated in this study. Range-finder doses have been determined for all samples, but standard measurement (i.e., OSL on pure quartz) has only been carried out on the samples with a Lund (Lund Luminescence Laboratory) ID number. For location in the sections, see Text-fig. 2.

Range-finder type	Stimulation wavelength	Stimulation temperature	Filter(s)	Preheat/ cutheat	Signal	Reference
RF-OSL	Blue (470 nm)	125°C	U340	220/180°C	post-IR OSL	Roberts and Wintle 2001
RF-IRSL	Infrared (870 nm)	125°C	Schott BG39	220/180°C	IRSL	Roberts and Wintle 2001
RF-IR50	Infrared (870 nm)	50°C	Schott BG39 and Corning 7-59	250/250°C	IRSL	Buylaert *et al.* 2009
RF-pIR225	Infrared (870 nm)	225°C	Schott BG39 and Corning 7-59	250/250°C	post-IR IRSL	Buylaert *et al.* 2009

Table 2. Detailed parameters of the four different range-finder types used in this study, determined by a combination of different stimulation and detection wavelengths and stimulation temperatures.

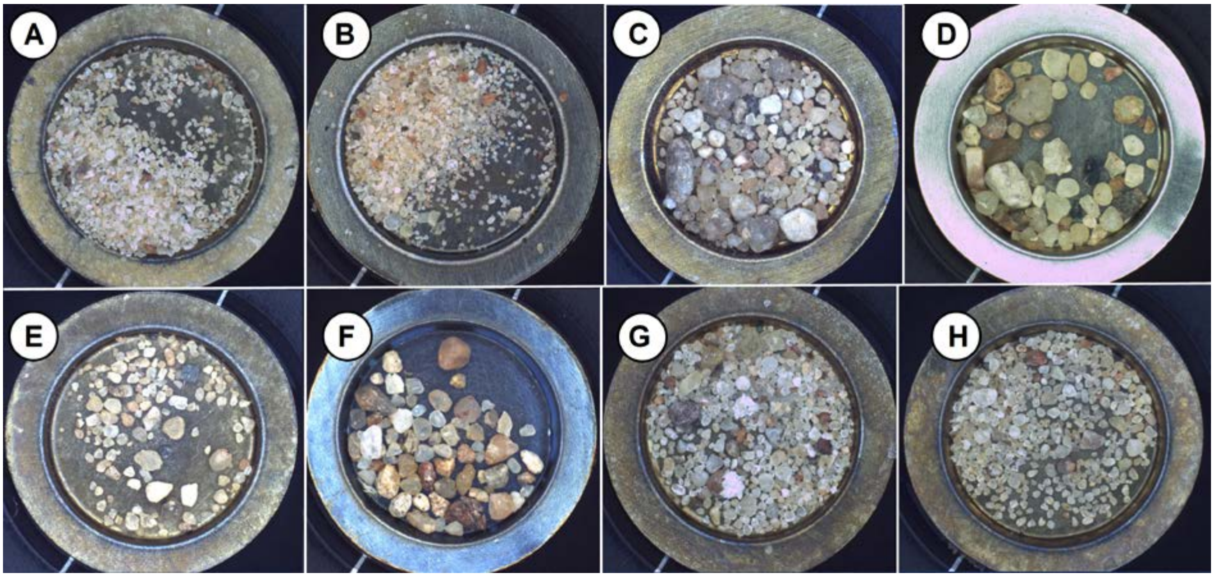

Text-fig. 3. Examples of aliquots with untouched (unprocessed) material taken directly from the sampling tubes. A, B – fine-sand grains; C, D – coarse- and medium-sand grains; E, F – tens of grains; G, H – hundreds of grains.

ment, a small amount (~0.1 g) of material was taken from the sampling tube under subdued red light in the Lund Luminescence Laboratory, Lund University, Sweden. The material was quickly dried at room temperature and placed in 11.7-mm stainless steel cups for measurement. This procedure follows the first main procedure recommended by Roberts et al. (2009). The material usually contained a mixture of finer (mostly sand; Text-fig. 3A, B) and coarser (gravelly; Text-fig. 3C, D) particles. The largest grains were manually removed from the cup. Nevertheless, some coarser grains were still present in part of the measured aliquots. Aliquot size ranged from ~60 grains (Text-fig. 3E, F) to hundreds of grains (Text-fig. 3G, H).

Three aliquots per untreated sample (Table 1) were analysed in a Risø TL/OSL reader model DA-20 (Bøtter-Jensen *et al.* 2010). Two double single-aliquot regeneration (SAR) protocols, adapted for quartz (Roberts and Wintle 2001) and feldspar (Buylaert *et al.* 2009), respectively, were applied resulting in four different measurement types (Table 2).

Twenty samples (Table 3) were fully processed for standard OSL dating at the Lund Luminescence Laboratory. Details of the preparation procedure and measurement can be found in Kalińska *et al.* (in press). In short, material from the central part of the sampling tube was wet-sieved and treated with HCl, H_2O_2 and HF, the latter for 40 min., as well as being density-separated to extract quartz grains in the 180–250 µm size range (Murray *et al.* 2021). Small (2-mm) single aliquots were measured in the same reader type with SAR protocols and preheat/cutheat temperatures of 260 ºC and 240 ºC, respectively for most samples. Between 17 and 41 aliquots were measured per sample.

The samples are divided into two datasets, where Dataset 1 consists of the 20 samples for which we have both SM-OSL doses and RF doses (Table 3), while Dataset 2 comprises the 16 samples for which we have RF doses only (Table 4). Dataset 1 functions as a training dataset and the results are then applied to Dataset 2.

RESULTS

Dataset 1: samples with known quartz doses

Quartz OSL doses obtained by standard measurement range from 20.2±1.2 Gy to 141±13 Gy (sample O2-OSL4 and P1-4, respectively; Kalińska *et al.* in press; W. Wysota, pers. com.) (Table 3). The range-finder doses have a spread from 12±3 Gy (RF-OSL for sample O2-OSL5) to 519±169 Gy (RF-IR225 for sample B1-3).

Plotting the different range-finder doses against the SM-OSL dose shows variable relationships (Text-fig. 4). Of the RF doses, the RF-OSL dose is on average the most similar dose to the SM-OSL dose (average RF-OSL/SM-OSL ratio 1.24) but the correlation is not strong ($R^2 = 0.39$; Text-fig. 4A), unless only the

Sample number	Lund ID	SM-OSL dose (Gy; Kalińska *et al.* in press; (W. Wysota, pers. com.)			RF-OSL dose (Gy)			RF-IRSL dose (Gy)			RF-IR50 dose (Gy)			RF-pIR225 dose (Gy)		
P1-1	19153	38.9	±	2.9	22	±	1	33	±	7	40	±	2	76	±	18
P1-2	19154	109	±	13	153	±	50	165	±	27	337	±	16	276	±	63
P1-3	19155	121	±	18	82	±	15	120	±	15	315	±	24	164	±	23
P1-4	19156	141	±	13	103	±	12	119	±	9	208	±	58	197	±	33
B1-1	19157	101	±	19	278	±	66	329	±	59	108	±	8	311	±	107
B1-2	19158	77.9	±	9.7	145	±	19	121	±	3	152	±	13	135	±	21
B1-3	19159	108	±	12	84	±	22	104	±	40	121	±	16	519	±	169
BW1-4-1	20029	114.5	±	7.5	122	±	10	128	±	6	324	±	90	418	±	108
BW1-4-2	20030	132	±	17	108	±	21	179	±	34	336	±	48	278	±	88
BW1-4-3	20031	92.7	±	9.2	145	±	11	185	±	18	213	±	98	258	±	41
SU1-1	20033	107	±	13	123	±	77	283	±	122	299	±	95	200	±	70
PLO1-2	20036	104	±	10	195	±	14	149	±	15	219	±	97	266	±	92
AT1-1	20037	92	±	10	134	±	15	192	±	30	226	±	1	234	±	28
AT1-2	20038	50.7	±	4.0	65	±	19	65	±	11	117	±	40	149	±	23
AT1-3	20039	62.9	±	4.2	99	±	7	145	±	20	123	±	29	194	±	45
AT2-3	20041	42.9	±	3.0	88	±	28	94	±	25	90	±	30	100	±	16
AT2-4	20042	30.4	±	1.6	28	±	4	37	±	7	132	±	83	124	±	68
AT4-3	20043	39.1	±	2.8	38	±	3	42	±	1	64	±	11	106	±	10
O2-OSL4	20048	20.2	±	1.2	17	±	4	14	±	0.3	22	±	2	21	±	2
O2-OSL5	20049	23.8	±	1.3	12	±	3	16	±	0.3	30	±	3	37	±	3

Table 3. Mean equivalent doses from quartz (SM-OSL doses) and range-finder mean equivalent doses (RF doses) from natural sediment for samples in Dataset 1. The SM-OSL doses are based on 17–41 aliquots per sample, while the range-finder doses are based on three aliquots per sample.

Sample no	RF-OSL dose (Gy)			RF-IRSL dose (Gy)			RF-IR50 dose (Gy)			RF-pIR225 dose (Gy)		
AIR1-1	367	±	164	178	±	29	200	±	26	196	±	93
AIR1-2	129	±	23	118	±	12	173	±	56	162	±	30
AIR1-3	94	±	40	117	±	51	156	±	55	147	±	39
AT3-1	109	±	15	128	±	22	286	±	46	268	±	88
AT3-2	138	±	17	170	±	14	87	±	11	194	±	103
AT3-3	105	±	54	120	±	16	103	±	3	270	±	66
AT4-1	104	±	25	132	±	27	84	±	37	94	±	23
AT4-2	24	±	2	30	±	3	31	±	2	125	±	24
AT1-5	23	±	15	71	±	21	75	±	28	144	±	16
BACH5-1	304	±	43	231	±	98	429	±	264	254	±	81
BACH5-2	182	±	14	195	±	26	364	±	65	243	±	59
PLK2-1	55	±	29	48	±	16	107	±	27	182	±	49
PLK2-2	47	±	31	22	±	4	37	±	2	56	±	14
PLK2-3	19	±	3	24	±	1	38	±	6	107	±	45
PLO1-3	59	±	14	97	±	39	77	±	14	61	±	36
SU2-1	30	±	6	57	±	33	80	±	4	73	±	4

Table 4. Range-finder mean equivalent doses (RF-doses) from natural sediment for the samples in Dataset 2 based on three aliquots per sample.

samples with low (<80 Gy) doses are considered (R^2 = 0.78; Text-fig. 4E). The strongest correlation is instead found for the RF-IR50 dose (R^2 = 0.68; Text-fig. 4C). All feldspar RF doses (RF-IRSL, -IR50 and -pIR225) have in general higher doses than the quartz OSL doses (average RF/SM-OSL ratios 1.50, 2.1 and 2.5, respectively). In all comparisons, the largest scatter is seen for high doses, some of which are also associated with large uncertainties (Text-fig. 4). For example, more than five-times higher doses are seen in RF-pIR225 than in quartz OSL (B1-3; Text-fig. 4D). A few outliers, both high and low, are also observed, for example the group of high outliers (>300 Gy) in RF-IR50 (Text-fig. 4C) and RF-OSL (B1-1; Text-fig. 4A). Outliers with high feldspar dose values are more common. In contrast, doses lower than 80 Gy show a trend that is more linear (Fig. 4E). Comparisons within the range-finder data show a strong correla-

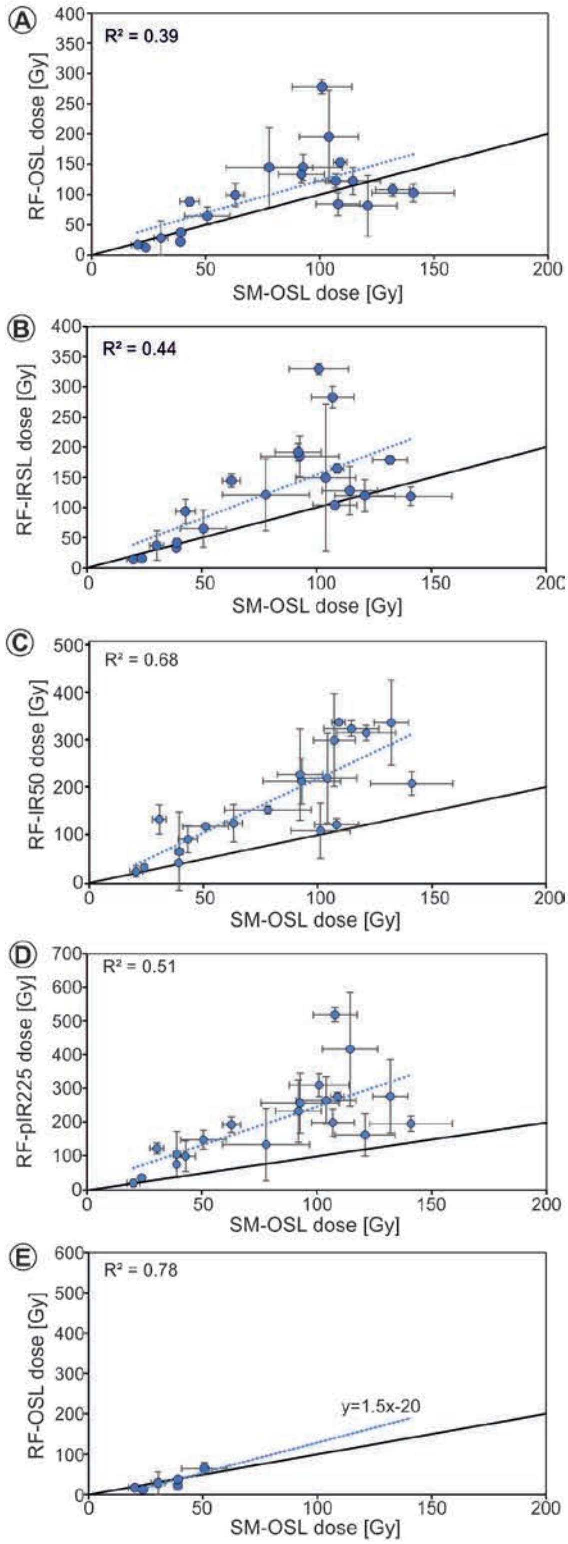

Text-fig. 4. Plots of the mean quartz equivalent dose (Gy) obtained by the SM versus the RF method. The black line is the 1:1 line. A – RF-OSL; B – RF-IRSL; C – RF-IR at low temperature of 50ºC; D – RF-pIR at temperature of 225ºC; E – RF-OSL with the low doses (<80 Gy) with formula to calculate the potential SM-OSL doses.

tion between RF-IRSL and RF-OSL doses ($R^2 = 0.75$; Text-fig. 5A) and very strong ($R^2 = 0.95$) when considering only the low-dose (<80 Gy) samples.

Dataset 2: samples with range-finder doses only

The remaining 16 samples, which do not have any known quartz OSL doses, have RF doses between 19±3 Gy (RF-OSL, sample PLK2_3) and 429±264 Gy (RF-IR50 sample Bach5-1) (Text-fig. 5A, B; Table 4).

The RF-OSL and RF-IRSL doses correlate strongly ($R^2 = 0.71$; Text-fig. 5B), similar to Dataset 1. A significant outlier is in the results with the highest doses (sample AIR1-1) with 367±164 Gy and 178±29 Gy for quartz and feldspar, respectively (Text-fig. 5B). Nevertheless, some large differences in the obtained measurements also appear in the low-dose samples, such as in sample AT1-5 (23±15 Gy and 71±21 Gy

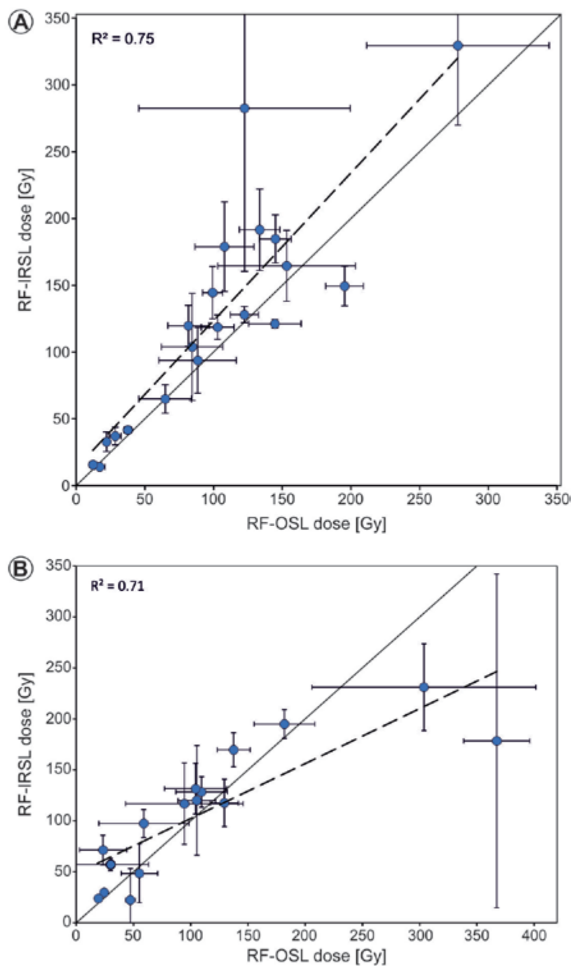

Text-fig. 5. Plots of the mean quartz equivalent dose (Gy) obtained by the RF-OSL method versus the mean feldspar equivalent dose (Gy) obtained by the RF-IRSL method. A – SM Dataset 1 (20 doses; Table 3); B – Dataset 2 without SM (16 doses; Table 4).

for quartz and feldspar, respectively). Interestingly, keeping only the low-dose samples (<80 Gy) does not improve the correlation but rather worsens it significantly ($R^2 = 0.16$), making it the poorest correlation in the analysed dataset. Similar is the case for the outlying low-dose samples. Retaining only the high-dose samples between ~80 Gy and ~200 Gy significantly improves the correlation up to $R^2 = 0.79$.

DISCUSSION

Correlation between the measurement types and the depositional environment context

Alexanderson and Bernhardson (2016) found that the equivalent doses of untreated polymineral material in the 1–60 Gy range using post-IR blue (RF-OSL) stimulation are on average as close as 96% of the doses determined on 180–250 µm pure quartz grains from aeolian sediments. For comparison, in the nine samples with low doses (<80 Gy) from Dataset 1 (20 samples) the average is 118%, with a wide range from 51% to 206% of the corresponding SM-OSL dose. For the whole Dataset 1, only six samples have RF-OSL doses within 20% of the SM-OSL dose (BW1-4-1, BW1-4-2, SU1-1, AT2-4, AT4-3, O2-OSL4; Table 3). These samples represent all types of sediment (Table 1). However, two samples from a periglacial and an aeolian environment (AT4-3 and O2-OSL4) have nearly identical SM-OSL and RF-OSL doses, suggesting a potential for successful RF-analysing of untreated material, and can be even used to estimate the 'real' doses.

The sand-wedge sample O2-OSL4 may contain well-bleached quartz particles from multiple sediment reworking events mixed with autochthonous deep-wedge material (Ateny 4 in Text-fig. 3A) post-dating the GLOF. The sediment reworking and transportation, which is observed at our sites, possibly involved pre-flooding sedimentation (1st stage), GLOF onset and peak discharge (2nd stage), its waning (3rd stage) and periglacial and aeolian grain reshaping (4th stage; Text-fig. 6) as suggested by the occurrence of the sand wedges and aeolian cover in places (W. Wysota, pers. com.). Sample O2-OSL4 likely experienced the 4th stage under periglacial conditions that provided material of good quartz luminescence properties. This sample seems as promising as the Swedish Dala sandstone that experienced some repeated transportation, which resulted in good luminescence properties of the sediment (Alexanderson and Bernhardson 2016). Besides the reworked aeolian environments, a range of recent glacifluvial environments with braid-bar-tail deposits and side-attached bar deposits has also been shown to carry good, best bleached quartz (King *et al.* 2014a).

In contrast, the worst correlation between the SM-OSL dose and the RF-OSL is found in sample B1-1 (101±19 Gy and 278±66 Gy, respectively; Table 3) at the topmost part of the Bryzgiel 1 section (Text-fig. 2A). This site is yet another megadune field south of the Wigry Lake (Text-fig. 1) but likely containing material delivered from a different source and hosting partly reworked GLOF sand (Weckwerth *et al.* 2019), which may account for the presence of poorly bleached quartz (Text-fig. 6).

Among the samples from Dataset 2 (with no SM-OSL) data, two of them (PLK2-3 and AT4-2) reveal good correlation between RF-OSLand feldspar RF (IRSL and IR50; Table 4), both in a range of the low-dose samples. This is not surprising considering our earlier findings: sample AT4-2 comes from same

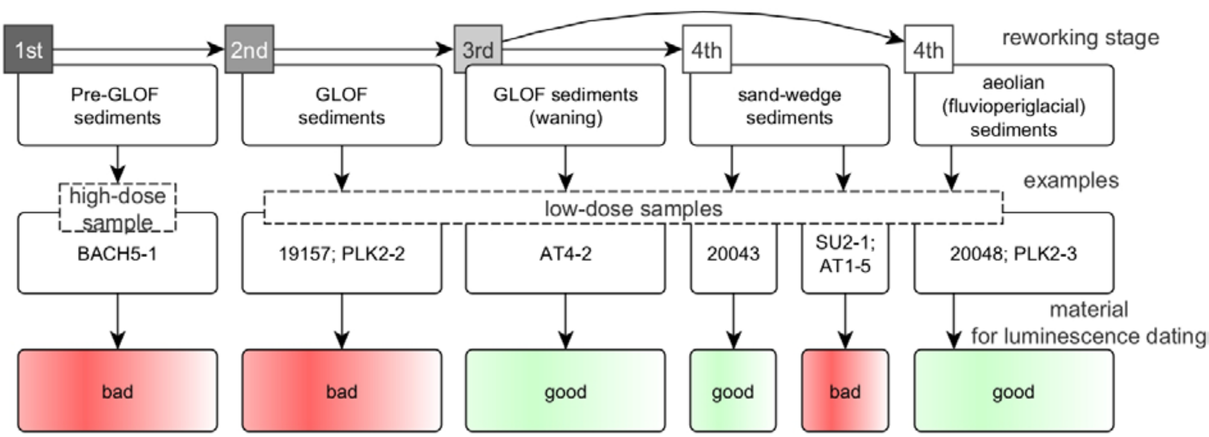

Text-fig. 6. Details on the sediment reworking stages in the study area along with examples of low- and high-dose samples, and inferences on whether quartz and feldspars are considered as potential material for luminescence dating based on their correlation characteristics.

Ateny 4 section as the sand-wedge sample AT4-3 (Text-fig. 2), and the former sample hosts sediments with multiple reworking and transportation history in a distal megadune. Also the PLK2-3 sample from the uppermost part of the Płaska section (Text-fig. 2) and the easternmost investigated megadune field (Text-fig. 1) reveals good correlation between the quartz and feldspar doses which might be again due to multiple reworking and sediment drying after the GLOFs (4^{th} stage; Text-fig. 6).

On the other hand, the neighbouring PLK2-2 sample carries quite a bad correlation with twice as high SM-OSL dose (47±31 Gy and 22±4 Gy for quartz and feldspar, respectively) among the low-dose samples, similar to the SU2-1 sample which also has a weak quartz-feldspar correlation. Whereas in sample PLK2-2 this poor correlation may be due to a limited sediment reworking during a GLOF (2^{nd} reworking; Text-fig. 6), the SU2-1 sample is more contentious. It comes from sand-wedge sediments (Text-fig. 2C) and is expected to be similar to the PLK2-3 sand-wedge sample (4^{th} reworking), which displays a very strong RF-OSL and RF-IRSL dose correlation as above stated. Multiple sediment reworking seems irrelevant for SU2-1; a more likely reason for the poor correlation between the RF-OSL quartz and the RF-IRSL doses in this sample is inclusion of allochthonous and unreworked material (Text-fig. 2C). The polymineral sand-wedge material in AT1-5 (Text-fig. 2A) is allochthonous too, because it carries a low value of RF-OSL (23±15 Gy; Table 4) among samples without the SM, and more than three-times the value of RF-IRSL (71±21 Gy; Table 4; Fig. 5B), and even more than six-times that of the RF-pIR225 (Table 4) giving the worst observed correlation. Several samples therefore do not follow the principle of a relatively good correlation in material with low doses, and the occurrence of unreworked sediments in sand-wedges may account for it.

Finally, some samples in the high-range doses also reveal large discrepancies. For example, the RF-OSL dose in sample AIR1-1 is twice as high as the RF-IRSL dose in this sample and in sample BACH5-1 (Table 4; Fig. 5B), which might be explained by a weak reworking of the GLOF and pre-GLOF sediment sequence documented at the Airfield and Bachanowo 5 sites, respectively.

Low versus high RF equivalent doses and their regional context

Application of RF allows a rapid assessment of equivalent doses (Roberts *et al.* 2009; Durcan *et al.* 2010) and in our study the RF helps in distinguishing between samples with low and high doses, which serves as a preliminary estimate of relative ages of the sediments. The RF can be used to constrain which OSL samples should be processed further with a conventional luminescence dating method to provide the real (and not partially bleached and overestimated) depositional ages.

If all samples come from the same region, from similar lithologies and have similar sediment dose rates (known e.g. from previous dating), the RF doses can be used to roughly estimate the relative age by dividing the measured equivalent dose by the dose rate. The average environmental dose rate for the samples in this study is ~2 Gy/ka (Kalińska *et al.* in press) for quartz, which is similar to the environmental doses of sediments in the region (between 1.16 Gy/ka and 3.31 Gy/ka, Kalińska *et al.* 2023). We therefore use a value of 2 Gy/ka as an average dose rate when estimating ages. This means that samples with quartz RF-OSL equivalent doses between 28 Gy and 65 Gy (Tables 3, 4) yield ages in the order of 15–30 ka, and possibly mark deposition at the end of the Weichselian glaciation when the GLOF took place (Weckwerth *et al.* 2019). Similarly, samples with lower RF-OSL doses between 12 Gy and 24 Gy (corresponding to *ca* 5–10 ka) would record some younger depositional events (post-GLOF) during the Holocene. Finally, samples with RF-OSL doses larger than 82 Gy (*ca* 40 ka) and as high as 367 Gy (*ca* 180 ka) are either incompletely bleached or older than the end of the Weichselian glaciation.

RF dose estimates based on the best correlation and their depositional environment context

We generally found poor agreement between RF-OSL and SM-OSL quartz, however considering only the low-dose samples (<80 Gy), significantly improved this correlation (up to $R^2 = 0.78$; Fig. 4E). In that case, the potential SM-OSL doses can be estimated from the relationship

$$f(x) = 1.5x - 20$$

where x refers to the RF-OSL value [Gy].

Applying the above relationship to the low-dose samples without the SM-OSL (PLK2-1, PLK2-2, PLO1-3) from two megadune sections (Płaska 2 and Płociczno 1; Text-fig. 1) yields recalculated doses of around 51–68 Gy (Text-fig. 7). Based on the sediment type, this dose range can be expected to mark GLOF events. One sample (SU2-1) from a broad sand-wedge in the Suwałki Utrata 2 section (Text-fig. 2C) gives

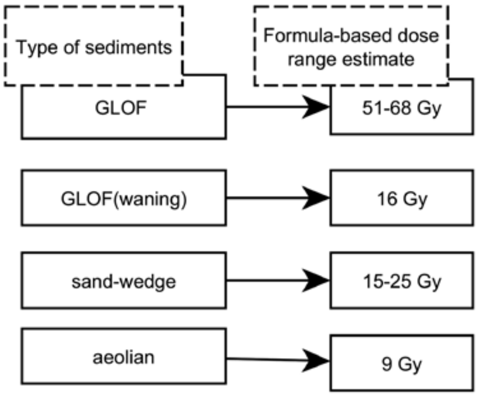

Text-fig. 7. The RF dose estimates for the low-dose samples without SM-OSL data.

a dose of ~25 Gy and sample AT4-3 from another wedge in the Ateny 4 section (Text-fig. 2A) gives a dose of 15 Gy, both suggesting post-GLOF periglacial deposition. The waning-flood sediments in the megadune section Ateny 4 have a similar dose of ~16 Gy. Finally, one sample (PLK2-3) with relatively low dose of 9 Gy possibly marks the Holocene aeolian activity in NE Poland.

Considering a reasonable correlation of 0.68 between the SM-OSL dose and the RF-IR50 dose (Fig. 4C), the latter can be additionally used as an age range estimator, similar to a promising luminescence signal found in dating extremely dynamic Late Holocene mass movement events (de Boer *et al.* 2023).

CONCLUSIONS

We tested 20 sediment samples with already known equivalent doses and 16 sediment samples with unknown doses using the luminescence dose range-finder method. The samples come from glacial meltwater, aeolian, and sand-wedge sediments in NE Poland. The range-finder is considered a tool to rapidly yield doses without time-consuming prior sediment preparation.

Our results reveal a minor number of samples with nearly identical doses obtained using standard quartz optically stimulated luminescence (OSL) and range-finder quartz OSL; these samples are of aeolian origin and represent multiply reworked sediments. Strong correlation between the standard OSL and range-finder quartz OSL doses depends on how many times the sediment was reworked, whereby several stages of reworking are considered as well-bleached and a good luminescence source. In the sand-wedge the materials are both suitable and less suitable. Material pre-GLOFs and GLOFs may account for the presence of poorly bleached quartz.

Testing several correlations between the standard quartz OSL and range-finder types helps to determine the best correlations, which may be used for age estimations. The best correlations are between the standard quartz OSL and range-finder feldspar infrared stimulated luminescence (IRSL) at 50ºC, and between the standard quartz OSL and range-finder quartz OSL in low-dose samples (<80 Gy). Considering this latter correlation, a formula that estimates a dose value can be used for new unprocessed samples. However, this formula and its dose recalculation from the range-finder quartz OSL to the standard quartz OSL must be treated very cautiously and considered together with the characteristics of the sediment type. The range-finder method estimates the range of dose, determines the low-dose and high-dose, and constrains the differences between the sampling sites but it is an approximation only, especially if a limited number of aliquots is measured. Considering this latter, it would be beneficial to measure more range-finer aliquots in order to obtain more accurate results to correlate with the standard OSL doses.

Acknowledgments

We would like to thank Edit Thamó-Bozsó and an anonymous reviewer for constructive comments that improved the manuscript. This study was carried out as part of a scientific project financed by the National Science Centre, Poland (project No. 2018/31/B/ST10/00976) and was supported by the project to develop international collaboration with the world's top academic institutions by members of Emerging Fields under the Excellence Initiative – Research University programme (project no: 90-SIDUB.6102.9.2021.PMEF1), the Research University – Initiative of Excellence: the Emerging Field 'Global Environmental Changes' and the 'CatFlood Research Team' at Nicolaus Copernicus University in Toruń, Poland.

REFERENCES

Alexanderson, H. and Bernhardson, M. 2016. OSL dating and luminescence characteristics of aeolian deposits and their source material in Dalarna, central Sweden. *Boreas*, **45**, 876–893.

Ber, A. 2006. Pleistocene interglacials and glaciations of north-eastern Poland compared to neighbouring areas. *Quaternary International*, **149**, 12–23.

de Boer, A.-M., Schwanghart, W., Mey, J., Adhikari, B.R. and

Reimann. T. 2023. Insight into the dynamics of a long run-out mass movement using single-grain feldspar luminescence in the Pokhara valley, Nepal. *Geochronology*, **6** (1), 53–70, preprint gchron-2023-12.

Bøtter-Jensen, L., Thomsen, K.J. and Jain, M. 2010. Review of optically stimulated luminescence (OSL) instrumental developments for retrospective dosimetry. *Radiation Measurements*, **45**, 253–257.

Burbidge, C.I., Sanderson, D.C.W., Housley, R.A. and Allsworth Jones, P. 2007. Survey of Palaeolithic sites by luminescence profiling, a case study from Eastern Europe. *Quaternary Geochronology*, **2**, 296–302.

Buylaert, J.P., Murray, A.S., Thomsen, K.J. and Jain, M. 2009. Testing the potential of an elevated temperature IRSL signal from K-feldspar. *Radiation Measurements*, **44**, 560–565.

Carling, P.A. 2013. Freshwater megaflood sedimentation: What can we learn about generic processes? *Earth-Science Reviews*, **125**, 87–113.

Denby, P.M., Bøtter-Jensen, L., Murray, A.S., Thomsen, K.J. and Moska, P. 2006. Application of pulsed OSL to the separation of the luminescence components from a mixed quartz/feldspar sample. *Radiation Measurements*, **41**, 774–779.

Durcan, J.A., Roberts, H.M., Duller, G.A.T. and Alizai, A.H. 2010. Testing the use of range-finder OSL dating to inform field sampling and laboratory processing strategies. *Quaternary Geochronology*, **5**, 86–90.

Dzierżek, J. and Zreda, M. 2007. Timing and style of deglaciation of north eastern Poland from cosmogenic ^{36}Cl dating of glacial and glaciofluvial deposits. *Geological Quarterly*, **51**, 203–216.

Herget, J., Agatova, A.R., Carling, P.A. and Nepop, R.K. 2020. Altai megafloods – the temporal context. *Earth-Science Reviews*, **200**, 102995.

Hu, G., Min, R., Zhou, Y., Yang, J., Wang, Y., Wang, C., Wang, H., Wang, P., Wang, L. and Fan, A. 2022. Luminescence dating of a megaflood event on a terrace of the Jinsha River, China. *Quaternary Geochronology*, **70**, 101303.

Kalińska, E., Weckwerth, P., Alexanderson, H. 2023. Recent advances in luminescence dating of the Late Quaternary sediments in the Baltic States, Northern Europe: A review. *Earth-Science Reviews*, **236**, 104272.

Kalińska, E., Weckwerth, P., Alexanderson, H., Piotrowski, J. and Wysota, W. (in press). OSL dating of glacial outburst flood deposits in NE Poland and their bleaching problem inferred from the landform-sediment associations and regional context. *Quaternary Research*.

King, G.E., Sanderson, D.C., Robinson, R.A. and Finch, A.A. 2014a. Understanding processes of sediment bleaching in glacial settings using a portable OSL reader. *Boreas*, **43** (4), 955–972.

King, G.E., Robinson, R.A.J. and Finch, A.A. 2014b. Towards successful OSL sampling strategies in glacial environments: deciphering the influence of depositional processes on bleaching of modern glacial sediments from Jostedalen, Southern Norway. *Quaternary Science Reviews*, **89**, 94–107.

Last, G.V. and Rittenour, T.M. 2021. Chronology of Missoula Flood Deposits at the Coyote Canyon Mammoth Site, Washington State, USA. *Quaternary*, **4**(3), 20.

Leighton, C.L. and Bailey, R.M. 2015. Investigating the potential of HCl-only treated samples using range-finder OSL dating. *Quaternary Geochronology*, **25**, 1–9.

Mahan, S.A., Rittenour, T.M., Nelson, M.S., Ataee, N., Brown, N., DeWitt, R., Durcan, J., Evans, M., Feathers, J., Frouin, M., Guérin, G., Heydari, M., Huot, S., Jain, M., Keen-Zebert, A., Li, B., López, G.I., Neudorf, C., Porat, N., Rodrigues, K., Sawakuchi, A.O., Spencer, J.Q.G., and Thomsen, K. 2023. Guide for interpreting and reporting luminescence dating results. *GSA Bulletin*, **135** (5–6), 1480–1502.

Marks, L. 2002. Last Glacial Maximum in Poland. *Quaternary Science Reviews*, **21**, 103–110.

Marks, L. 2012. Timing of the Late Vistulian (Weichselian) glacial phases in Poland. *Quaternary Science Reviews*, **44**, 81–88.

Munyikwa, K., Kinnaird, T. C. and Sanderson, D. C.W. 2021. The potential of portable luminescence readers in geomorphological investigations: a review. *Earth Surface Processes and Landforms*, **46** (1), 131–150.

Murray, A.S. and Wintle, A.G. 2000. Luminescence dating of quartz using an improved single-aliquot regenerative-dose protocol. *Radiation Measurements*, **32**, 57–73.

Murray, A., Arnold, L.J., Buylaert, J.-P., Guérin, G., Qin, J., Singhvi, A.K., Smedley, R. and Thomsen, K.J. 2021. Optically stimulated luminescence dating using quartz. *Nature Reviews Methods Primers*, **1**, 72.

Roberts, H.M., Durcan, J.A. and Duller, G.A.T. 2009. Exploring procedures for the rapid assessment of optically stimulated luminescence range-finder ages. *Radiation Measurements*, **44**, 582–587.

Roberts, H.M., Wintle, A.G. 2001. Equivalent dose determinations for polymineralic fine-grains using the SAR protocol: application to a Holocene sequence of the Chinese Loess Plateau. *Quaternary Science Reviews*, **20**, 859–863.

Sanderson, D.C.W., Bishop, P., Houston, I. and Boonsener, M. 2001. Luminescence characterisation of quartz-rich cover sands from NE Thailand. *Quaternary Science Reviews*, **20**, 893–900.

Sanderson, D.C.W., Bishop, P., Stark, M.T. and Spencer, J.Q. 2003. Luminescence dating of anthropogenically reset canal sediments from Angkor Borei, Mekong Delta, Cambodia. *Quaternary Science Reviews*, **22**, 1111–1121.

Sanderson, D.C.W. and Murphy, S. 2010. Using simple portable OSL measurements and laboratory characterisation to help understand complex and heterogeneous sediment sequences for luminescence dating. *Quaternary Geochronology*, **5** (2–3), 299–305.

Spooner N.A. 1994. The anomalous fading of infrared-stimulated luminescence from feldspars. *Radiation Measurements*, **23**, 625–632.

Stone, A., Bateman, M.D. and Thomas, D.S.G. 2015. Rapid age assessment in the Namib Sand Sea using a portable luminescence reader. *Quaternary Geochronology*, **30**, 134–140.

Stone, A., Bateman, M.D. and Thomas, D.S.G. 2016. Rapid assessment of Namib Sand Sea sediment chronologies? Testing a portable luminescence reader against full OSL dating. *Quaternary International*, **404**, 200–201.

Thomsen, K.J., Jain, M., Murray, A.S., Denby, P.M., Roy, N. and Bøtter-Jensen, L. 2008. Minimizing feldspar OSL contamination in quartz UV-OSL using pulsed blue stimulation. *Radiation Measurements*, **43**, 752–757.

Wallinga, J. 2002. Optically stimulated luminescence dating of fluvial deposits: a review. *Boreas*, **31** (4), 303–322.

Weckwerth, P., Przegiętka, K.R., Chruścińska, A. and Pisarska-Jamroży, M. 2013. The relation between optical bleaching and sedimentological features of fluvial deposits in the Toruń Basin (Poland). *Geological Quarterly*, **57** (1): 31–44.

Weckwerth, P., Wysota, W., Piotrowski, J.A., Adamczyk, A., Krawiec, A. and Dąbrowski, M. 2019. Late Weichselian glacier outburst floods in North-Eastern Poland: Landform evidence and palaeohydraulic significance. *Earth-Science Reviews*, **194**, 216–233.

Weckwerth, P., Kalińska, E., Wysota, W., Krawiec, A., Adamczyk, A. and Chabowski, M. 2022. What does transverse furrow train in scabland-like topography originate from? The unique records of upper-flow-regime bedforms of a glacial lake-outburst flood in NE Poland. *Quaternary International*, **617**, 40–58.

Wintle A.G. 1973: Anomalous fading of thermoluminescence in mineral samples. *Nature*, **245**, 143–144.

Wintle, A.G. and Adamiec, G. 2017. Optically stimulated luminescence signals from quartz: A review. *Radiation Measurements*, **98**, 10–33.

Woronko, B. and Dąbski, M. 2023. The North European Plain. In: Oliva, M., Nývlt, D. and Fernández-Fernández, J.M. (Eds), Periglacial Landscapes of Europe, 281–322. Springer; Cham.

Yang, A., Wang, H., Liu, W., Hu, K., Liu, D., Wu, C. and Hu, X. 2022. Two megafloods in the middle reach of Yarlung Tsangpo River since last-glacial period: Evidence from giant bars. *Global and Planetary Change*, **208**, 103726.

Manuscript submitted: 5th April 2024
Revised version accepted: 18th October 2024